



Published in final edited form as:

Cancer Gene Ther. 2011 April ; 18(4): 265–274. doi:10.1038/cgt.2010.77.

Pre-clinical toxicity assessment of tumor-targeted interleukin-12 low-intensity electrogenetherapy

Scott Douglas Reed, DVM¹ and Shulin Li, PhD²

¹Department of Comparative Biomedical Sciences, LSU School of Veterinary Medicine, Skip Bertman Drive, Baton Rouge, LA 70803. 225-578-9755 (O)

²Department of Pediatrics Research, UT MD Anderson Cancer Center, UT Graduate School of Biomedical Sciences, 1515 Holcombe, Houston, TX 77030

Abstract

This study's goal was to assess the safety of tumor-targeted interleukin-12 (ttIL-12) when administered by electrogenetherapy in C3H/HeJ mice by identifying an initial safe dose for human dose escalation schemes, toxicity target organs, markers of toxicity, and toxicity reversibility. Tumor-free mice receiving two doses of 0.45% NaCl, 1 µg ttIL-12 DNA in 0.45% NaCl, or 5 µg ttIL-12 DNA in 0.45% NaCl ten days apart combined with low-intensity electroporation were compared to non-treatment controls over time. All mice had blood cell counts, serum chemistry profiles, plasma IL-12 and IFN γ determinations, necropsy, and multi-organ histopathology. Mild treatment-associated changes included electroporation-associated muscle changes that resolved by 30 days; decreased total white blood cell counts and infectious disease in the 5 µg ttIL-12 group, but not in the 1 µg group; and liver changes in ttIL-12 groups that correlated with alanine transaminase (ALT) levels and resolved by 30 days. Dystrophic cardiac calcification seen in older, 5 µg ttIL-12-treated mice was the only serious toxicity. Based on these results and the lack of any effect on wound healing when combined with surgery, low-intensity electrogenetherapy with ttIL-12 appears to be safe and well tolerated.

Keywords

Gene therapy; IL-12; tumor targeting; toxicity; cancer; electroporation

INTRODUCTION

One of the major challenges associated with traditional surgical oncology, radiation, and chemotherapy is tumor recurrence and metastasis. One strategy to prevent tumor recurrence and metastasis is to induce or augment anti-tumor immunity. Interleukin 12 (IL-12) induces and maintains a powerful Th1-mediated anti-tumor immune response and has been used therapeutically in humans to treat neoplasia. The major effects of IL-12 are the stimulation of IFN- γ production by natural killer (NK) and T cells, which in turn stimulates additional IL-12 production¹, and induction of anti-angiogenesis genes². Another important role of IL-12 is to exhibit immunoregulatory functions in the generation of T helper 1 (Th1) and cytotoxic T lymphocytes (CTL)³. For these reasons, daily systemic administration of IL-12 recombinant protein (rIL-12) has been shown to generate a significant inhibitory effect on

²Correspondence: Shulin Li (sli4@mdanderson.org).

CONFLICT OF INTEREST STATEMENT:

The authors declare no conflict of interest.

the metastatic tumor growth of B16F10 melanoma, established murine renal carcinoma (RENCA), and CT26 tumors^{2, 4, 5}. Unfortunately, rIL-12 has also been associated with significant adverse effects, including death^{6, 7}. Investigation of rIL-12 toxicity suggests that cytokine-induced shock causing early deaths was mediated by NK cell production of IFN γ ⁸. Much of this toxicity was attenuated by giving low, “desensitizing” doses of rIL-12 prior to treatment with the normal dose regimen; nevertheless, use of rIL-12 has now been supplanted by use of IL-12 gene therapy for cancer treatment.

Systemic administration of cytokines at pharmacologic doses results in high concentrations of cytokines in the circulation and often in suboptimal levels in tissues at the site of tumors, therefore therapy is more likely to cause systemic toxicity and less likely to be efficacious in treating the primary tumor. In contrast, EP-mediated cytokine gene transfection allows localized expression of cytokine at targeted sites, avoiding deleterious side effects and resembling the normal paracrine effect of cytokines. This localized effect can be enhanced more, if the gene is somehow targeted to specific tissue or the tumor itself.

Our laboratory has previously demonstrated and published the efficacy of intratumoral EP of the gene for IL-12⁹. Others have also found that therapy using the gene for IL-12 is safe and effective in a variety of pre-clinical models along with in human phase 1 trials treating melanoma¹⁰. However, in these safety trials B16 tumor-bearing mice were used, making it difficult to extrapolate to IL-12 cancer gene therapy in general (and making it difficult to rule out variables associated with tumor burden). Moreover, the electroporation field in those studies was a much higher voltage (1300 V/cm) and shorter duration (95 μ sec) than the parameters used in this study¹¹. Our laboratory and others have found that lower voltage, longer duration pulses are associated with comparable transfection efficiency in a variety of mouse tumor models using standard reporter gene assays¹²⁻¹⁴. Additionally, currently available commercial electroporators deliver low voltage over longer intervals.

Safety of EP has also been examined in numerous studies and numerous EP protocols have been found to be safe and effective for most commonly used tissues¹⁵⁻¹⁷. There is some concern regarding use of EP in heart muscle, and patients with defibrillators or arrhythmias may not be good candidates for EP¹⁷. To our knowledge, nobody has examined the toxic effects of EP over time when applied under clinical conditions in a systematic way, nor has anyone reported the safety and toxicity of a relatively low voltage, long duration electroporation protocol; therefore we sought to characterize EP changes at numerous acute and a chronic end-points using a clinical electroporator to determine if there was severe or lasting toxicity.

To increase the efficacy of anti-tumor immune induction and further address the concern of safety, we have developed a plasmid DNA vector encoding a tumor-targeted peptide linked to the IL-12 gene, allowing the gene product to preferentially accumulate in tumors regardless of the site of injection. Pre-clinical therapeutic studies using murine ttIL-12 encoding plasmid have been completed in four independent tumor models; we have found that accumulation of IL12 protein in tumors is safe and triggers a more aggressive anti-tumor immune response than systemic rIL-12 therapy (Cutrera, submitted manuscript). In this study, the safety and toxicity of ttIL-12 was thoroughly analyzed (according to FDA guidelines for Investigational New Drug (IND) approval) in order to determine whether this novel fusion gene can be safely used in humans under clinical circumstances.

Materials & Methods

GLP or GLP-like protocols

Serum chemistries and complete blood counts (CBCs) were performed by Antech Diagnostics (Memphis TN), which is fully compliant with Good Laboratory Practice (GLP) Regulations as set forth in 21 CFR Part 58 as well as other regulatory requirements. All other procedures, including tissue archival, quality control, and data keeping procedures were conducted in GLP-like conditions (as stipulated by GLP regulations, but not certified by the Food and Drug Administration (FDA)).

Mice

All animal use studies had approval from the Louisiana State University Institutional Animal Care and Use Committee (Baton Rouge, LA). This committee follows USPHS Policy on Humane Care and Use of Laboratory Animals. Young adult male and female C3H/HeJ mice were obtained from a commercial vendor (Harlan Laboratories, Inc., Indianapolis, Indiana), were fed *ad libitum* a standard diet (Harlan Teklad irradiated mouse diet 7912, Madison, WI), and were housed in a temperature-controlled animal facility with a 12/12-hour light/dark cycle. Each group for the toxicity studies consisted of six male and six female mice; the age of mice at the time of the first treatment in this study was 8.5 weeks.

Cell lines and propagation

For tumor resection and wound healing studies, SCCVII murine squamous cell carcinoma cells which are syngeneic in C3H mice, originally obtained from Dr Bert O'Malley (Baylor College of Medicine) were maintained as monolayers in Dulbecco's Modified Eagle Medium. Tumors from study mice were harvested and confirmed to be spindleoid squamous cell carcinoma cells based on routine histopathology, cytokeratin immunohistochemistry, and transmission electron microscopy. Cells were harvested from flasks using trypsin-EDTA (0.05% trypsin-0.53 mmol/L EDTA; Mediatech), collected by centrifugation, and washed. Cells were counted and their concentration was adjusted to 2×10^5 cells/ml using sterile phosphate-buffered saline (PBS) prior to inoculation into mice.

Tumor inoculation and monitoring

Tumor cells were inoculated in syngeneic C3H mice by intradermal injection of SCCVII cells in the caudodorsal skin. 30 μ l of approximately 2×10^5 SCCVII tumor cells in sterile PBS was delivered to each mouse. Tumors were monitored using a digital vernier caliper and volumes were calculated using the formula $4/3\pi(a^2 b)$ where "a" is the tumor long dimension (diameter) and "b" is the shortest measurement perpendicular to "a".

Anesthesia

For all procedures requiring anesthesia, mice were anesthetized by chamber induction with 4% isoflurane in oxygen and were subsequently maintained by mask administration of isoflurane in oxygen to effect. During longer procedures, an infrared heat lamp was used for thermal support. Respiratory effort and rate along with anal tone and withdrawal reflexes were monitored throughout anesthesia.

Tumor resection surgery

When tumor areas averaged 30,000 mm³, mice were anesthetized, the area surrounding the tumor was clipped to remove hair, and the surgical site was prepared with three alternating 70% ethanol/2% chlorhexidine scrubs. The site was draped with a sterile drape and an elliptical incision was made with minimal tumor margins (approximately 1 mm – no effort

was made to completely excise tumors beyond a minimal margin) and the tumor was removed. The skin defect was closed with 2–3 cruciate sutures of 5-0 silk.

Plasmid

DNA encoding the tumor-targeting peptide (CHP) was inserted into the murine IL-12 gene construct immediately upstream to the p40 termination codon (Cutrera, submitted manuscript). This gene construct expressed CHP-IL-12, herein referred to ttIL-12, and was inserted into a pCLneo mammalian plasmid expression vector (Promega Corporation, Madison, Wisconsin).

Electroporation

Either skin overlying the dorsal lumbar epaxial musculature or quadriceps femoris muscle were electroporated using a fixed-voltage, four-needle array disposable electrode with a 4 mm gap delivering two 60 ms pulses of 46 V (200 V/cm) spaced approximately 190 ms apart, attached to a Medpulsar™ (Inovio Incorporated, San Diego, California) clinical electroporator. For SC application (the first treatment), either 30 μ L of 0.45% saline or ttIL-12 in 0.45% saline were injected subcutaneously; within 15–20 seconds the electrode was inserted transcutaneously straddling the injection site; and the pulses were delivered. For IM use, the same volume was injected bilaterally in the quadriceps muscles (the total volume was therefore 60 μ L, and the total DNA was divided between the two limbs), followed by insertion of the electroporator needles deep into the musculature surrounding the injection site.

Toxicity study

Groups of six female mice and six male mice divided equally between no treatment controls, 0.45% NaCl EP, 1 μ g ttIL-12 DNA in 0.45% NaCl, and 5 μ g ttIL-12 DNA in 0.45% NaCl were treated. The volumes injected were 30 μ L in the case of SC treatment and 60 μ L divided bilaterally into two 30 μ L aliquots for IM treatment. Treatment consisted of initial SC EP followed ten days later by IM EP. Control and treatment groups were then sacrificed at acute time points (1, 3, and 7 days) and a 30 day chronic time point.

Dosages of ttIL-12 were a presumably toxic mega-dose of 5 μ g IL12 DNA and a therapeutic dose of 1 μ g IL-12 DNA. The presumed toxic dose was chosen for determining the toxicity limit but will not be translated to humans because it would equal an impractical 22.5 mg in a 90 kg human (requiring a minimum injection of approximately 25 mL). The therapeutic dose chosen as most likely to be translated into human trials, is 1 μ g for multiple administrations, which is equal to 4.5 mg in a 90 kg human.

Surgery augmented with ttIL-12 EP study

To examine the effect of ttIL-12 EGT on recovery from tumor resection surgery, groups of six male mice were treated with the aforementioned protocol, but a massive dose of 20 μ g of ttIL-12 was administered during each episode of EGT.

Physical exam/behavior monitoring

A brief physical exam including body weight, respiratory rate and effort, mucus membrane character, cutaneous lesions, musculoskeletal changes, and localized tissue damage was performed on each mouse the day after EP and every seven days thereafter. Mice were also monitored for gait abnormalities and grooming behavior along with any other detectable behavioral anomalies.

CBC & chemistry analysis

Mice were anesthetized and the brachial artery was accessed through an incision created in the ventral axilla; the artery was severed and pooled blood was collected with a sterile glass pipette. Approximately 400–600 μ l of blood was collected into a miniature EDTA tube (BD Microtainer™ Tubes, Becton, Dickinson and Company) and mixed well. The remaining blood – usually approximately 800 μ L – was collected into a miniature plasma separator tube (BD Microtainer™, Becton, Dickinson and Company) and thoroughly mixed. A blood smear was made from the EDTA blood sample and the remaining blood and plasma were sent to a private GLP lab (Antech Diagnostics, Memphis, Tennessee) for a CBC and select chemistry analysis.

Euthanasia and gross necropsy

Under isoflurane general anesthesia, mice were exsanguinated and death was assured through cervical dislocation. All mice received a complete necropsy. Any tissue which had gross lesions (in addition to those routinely collected) was saved and processed for histopathologic examination.

Histopathology

All major perfused organs as well as any tissues with lesions (2 sections of skin) were fixed in 10% neutral-buffered formalin. Routine tissues examined histologically on all mice were liver, spleen, kidneys, lungs, heart, thymus, tracheobronchial lymph nodes, brain, bone marrow (lumbar spine & femurs), and quadriceps musculature. After fixation the tissue was cut-in, embedded in paraffin, sectioned on a microtome, mounted on glass slides, and stained with hematoxylin and eosin. Cover-slipped slides were examined by a pathologist and lesions were recorded. All slides and paraffin blocks were subsequently archived.

Statistical Analysis

Groups in each phase of evaluation were compared to control mice using a two-tailed T-test with a confidence interval of 95%. Charts of group means include standard error bars unless indicated otherwise.

RESULTS

Optimization of Medpulsar™ parameters

Our ultimate goal is to effectively deliver ttIL-12 gene to tumors, tissues at the margins of tumors, or systemically via musculature using EP in order to prevent tumor recurrence after primary tumor ablation. To achieve this goal, it is important to have a set of EP parameters enhancing gene delivery in multiple tissues. To determine such a set of parameters, we compared each of the clinically used applicators provided by the manufacturer (Inovio, San Diego, California) of the electroporator used in this study. We found that using the Medpulsar™ fixed-voltage applicator delivering 107 V/cm for two consecutive 60 msec pulses separated by a pause of approximately 190 msec allowed statistically significant ($p = 0.002$ and $p < 0.001$) high levels of reporter gene and cytokine expression when delivered both SC and IM (Fig. 1A). This applicator delivers 46 V across a 4 mm gap, four-needle electrode array that is inserted transcutaneously.

Cytokine expression after ttIL-12 EGT

In previous use of rIL-12, toxicity of IL-12 protein was seen with a large systemic acute dose of rIL-12. It is generally agreed that low constitutive IL-12 expression kinetics are produced by IL-12 EGT and one of the advantages of EGT is local expression without significant, potentially toxic systemic levels of cytokine. To determine whether clinical

application of the optimized EP parameters with ttIL-12 yielded the safe expression kinetics, we determined plasma cytokine levels in all of the sacrificed mice. The previously determined parameters yielded efficient transfection of the gene for ttIL-12 in vivo using the Medpulsar™ as indicated by detection of significant plasma cytokine levels only in IL-12 DNA-treated mice (Fig. 1B & 1C), yet we found no statistically significant elevation in systemic plasma cytokine levels. Mean levels of IL-12 p70 protein peaked at about 600 pg/mL in the 5 µg dose group on day three, and at approximately 60 µg/mL in the 1 µg therapeutic dose group on day seven. Levels of IFN γ also increased after treatment, with the mean peak value reaching approximately 120 pg/mL on day seven in the 5 µg treatment group, and approximately 360 pg/mL in the 1 µg treatment group.

Thus, EP parameters using the Medpulsar™ electroporator and four-needle electrode array were effective in numerous reporter genes and for therapeutic ttIL-12. As expected, systemic levels of IL-12 were not significant enough to potentially cause systemic toxicity. Additionally, levels of IL-12 were greater in the higher dose group – particularly on day three. The results for IFN γ were similar, but higher levels were seen in the low dose IL-12 group compared to the high dose group at acute time points. It is possible that IFN γ production was higher in the lower dose ttIL-12 group because of greater attenuation of IFN γ response by the high dose of ttIL-12, similar to the desensitizing dose of rIL-12 used to prevent IFN γ shock and fatality in rIL-12 therapy⁷. Unfortunately, to achieve significance and make any definitive conclusions, a greater number of mice would be required.

Background lesions in C3H/HeJ mice over time

Since all major perfused organs were evaluated histologically, we also noted lesions that appeared to have no relation to ttIL-12 EGT therapy. Two minor changes were noted over time in all groups (without increased severity or incidence in any particular treatment group). The incidence of bronchial-associated lymphoid tissue hyperplasia increased over time and was unassociated with treatment (presumably because of environmental inhalant antigen exposure). Additionally, the incidence of incisor malocclusion and overgrowth increased as mice aged. Lymphoid hyperplasia of lymph nodes, thymus and spleen were noted in all mice (both treatment and controls) throughout the study; and splenic extramedullary hematopoiesis, a common frequent finding in mice, was constant between groups and over time.

Local effects of electroporation

In order to determine the local effects of electroporation, muscle and skin were harvested from electroporation sites and examined microscopically. Focal to multifocal acute rhabdomyocyte necrosis with subsequent pyogranulomatous to granulomatous myositis followed by myoregeneration and resolution were seen at site of needle electrode insertion in numerous mice in all of the groups that received IM EP (Fig. 2). The incidence of detectable muscle damage peaked at seven days for the ttIL-12 treated mice, and was maximal on day 1 for the 0.45% saline treated mice. These trends may reflect the more widespread tissue inflammation over time and chances of detecting a change, more than reflecting increasing severity; in fact, by day 30, no muscle lesions were detected except for a single small focus of muscle degeneration, myofiber loss, and mineralization in a mouse of the 5 µg ttIL-12 treatment group (in a mouse that also had marked DCC).

We also monitored behavior and performed periodic physical examinations of the mice after EP and found that several mice were transiently lame in one or both pelvic limbs after IM EP. Mice that were lame were rechecked periodically and clinically detectable lameness

resolved completely in all mice by seven days after IM EP. There was not relationship between the incidence or severity of lameness and the substance injected.

Liver toxicity from ttIL-12

The biggest concern regarding adverse effects from IL-12 was hepatotoxicity; therefore several lobes of liver were examined histologically for ttIL-12 EGT lesions and a scoring system was used to document severity and incidence of lesions in different treatment groups (Fig. 3). There was a mild increase in the detection of liver lesions over time in the two ttIL-12 treatment groups, but none seen in either the control mice or the 0.45% saline treated mice (Fig. 3). Although none of the toxicity appeared serious, the most severe lesions, and the highest incidence of lesions, were seen on day seven (Fig. 3). Lesion incidence and severity were also greater in the 5 μ g ttIL-12 treatment group than in the 1 μ g ttIL-12 treatment group, but had essentially resolved by day 30.

To determine if there were any serologic indicators of liver toxicity and to see if these analytes correlated with histologic lesions, we compared mean levels of alanine transaminase (ALT) and alkaline phosphatase (ALP) activity in each group as well as levels of albumin (ALB) (Fig. 3). For alkaline phosphatase and albumin, there was no significant difference between treatment groups or over time. For ALT, there was a mild, but statistically insignificant ($p < 0.05$), increase in treatment group deviation from controls up to day seven, which returned to normal by day 30. Levels never reached clinically relevant increases (2–3 fold higher than normal range), and levels of ALT in saline treatment groups were essentially as high as or higher than in the ttIL-12 treatment groups. Nevertheless, ALT levels did correlate with liver toxicity on an individual animal basis and is thought to be a good monitoring parameter for acute liver toxicity.

Systemic immune effects of ttIL-12 EGT

In order to determine if there were any significant systemic effects of ttIL-12 EGT on the hematopoietic system and systemic immunity, CBCs and bone marrow histology were evaluated. In the case of WBC, there was a trend to decreasing total counts up to day seven which returned to normal by day 30 (Fig. 4). The trend was not significantly different from control mice in the 1 μ g treatment group ($p = 0.053$ on day 3 and $p = 0.109$ on day 7), but was in the 5 μ g treatment group ($p = 0.017$ on day three and $p = 0.023$ on day seven). The incidence of infectious disease was essentially non-existent (except possibly for mild BALB hyperplasia) in all groups except for the 5 μ g ttIL-12 treatment group, which had two mice on day 30 that had severe, potentially life-threatening, infectious diseases. One mouse had a moderate to severe, multifocal to coalescing, pyogranulomatous cholangiohepatitis (Fig. 4B), and the other mouse had severe, bilateral, subacute to chronic, diffuse, pyogranulomatous pyelonephritis (Fig. 4C). Of note is the fact that the second mouse also was one of the mice with DCC. No effects on bone marrow or other hematopoietic parameters were noted.

Dystrophic cardiac calcification

In histologically evaluating all other organs for potential ttIL-12 EGT toxicity, the only other major change seen in any of the mice was seen in the day 30, 5 μ g ttIL-12 treatment group, which had 3 mice (25%) with moderate to severe DCC (Fig. 5). Of these mice, one died, and one had evidence of biventricular congestive heart failure (pulmonary edema with splenic and hepatic congestion) at the time of sacrifice.

As noted above, the only fatality in the 192 mice of this study was a female in the mega-dose 5 μ g chronic 30 day group that died on day 22 after the IM EGT treatment. The cause of death in this mouse was thought to be biventricular congestive heart failure secondary to

DCC. Aside from severe myocardial mineralization (similar to Fig. 5B, but more severe), this mouse had hepatosplenomegaly due to congestion and mild hemosiderosis in the liver, spleen, and lungs. In the lungs, numerous alveolar macrophages contained either erythrocytes or hemosiderin (“heart failure cells”), and the interstitial spaces surrounding major vessels were expanded. Definitive evidence of pulmonary alveolar edema was not seen, but the interval between death and post-mortem examination was estimated to be 12–24 hours. The female mouse with the heart depicted (Fig. 5B) was also in congestive heart failure at the time of sacrifice as evidenced by pulmonary edema along with hepatic and splenic congestion.

Effect of ttIL-12 EGT on wound healing

Because we anticipate combining ttIL-12 EGT with surgical resection of primary tumors, analysis of wound healing when ttIL-12 EGT was critical for assuring that the therapy did not interfere with surgical protocols. Therefore, we grossly evaluated wound healing after EGT and tumor resection in squamous cell carcinoma tumor-bearing C3H mice and compared with wound healing in non-treatment controls. The last figure depicts healed tumor resection incisions seven days after surgery in mice treated with two treatments of 20 µg ttIL-12 prior to surgery (Fig. 6a & 6b). Wound healing was subjectively evaluated by observing the time to complete wound epithelialization (n =5 mice per group). As can be seen from the plot comparing wound epithelialization times (fig. 6c), EGT treatment with massive doses of ttIL-12 produced no statistical difference (p=0.5415) in primary intention wound re-epithelialization.

DISCUSSION

Several clinical trials are beginning or underway in humans using EP to deliver DNA in the form of vaccines or therapeutic genes; however, only one toxicology study was found in the literature using tumor-bearing mice to examine the safety of IL-12 gene EGT¹¹. Furthermore, the aforementioned study used high voltage (1,300 V/cm), short duration (0.1 msec) EP pulses in contrast to the low voltage (107 V/cm), long-duration (60 msec) pulses used in the current study. The electrode array used was also different than the one used in this study (a six-needle array versus the current four-needle array).

Comparing the different EP parameters, we did find effective transfection using the current parameters (Fig. 1), but it was important to also determine if these EP parameters caused any serious adverse effects. In addition to establishing the safety of the current set of EP parameters, it was also important to establish the safety of ttIL-12. Theoretically, a tumor-targeted gene should be both safer and more efficacious than a systemically-administered, non-targeted gene. As expected, therapeutic use of ttIL-12 EGT was found to be safe and well tolerated under conditions likely to be used for EGT clinically (Figs. 2, 3, & 4).

To our knowledge, this is also the first large scale study of IL-12 toxicity in non-tumor bearing mice, and the first examining the effects of relatively low voltage, long duration EP pulses. Tumor-bearing mice are not normal immunologically^{18–20}, so extrapolation from studies in tumor-bearing mice is fraught with a number of variables which may affect toxicity and efficacy of immune therapy. Additionally, both transfection efficiencies and local EP effects vary widely depending on the EP system used.

Using these parameters, local muscle changes in response to EP were completely resolved by day 30. Interestingly, damage was more frequently detected on days one and three in the group treated with carrier only – perhaps because of the hypotonic osmolarity of the half-strength saline compared to DNA solutions. A protective effect of ttIL-12, other than adding colloidal pressure, seems unlikely at these acute time points but cannot be ruled out.

Although the damage was detectable, albeit transient, these changes should be viewed with the perspective that inserting the 4 mm wide, four electrode array into mouse quadriceps affected a much greater muscle mass than would be commonly used in humans – perhaps this would be analogous to penetrating human thighs with four equidistant railroad spikes spaced 25–50 cm apart and applying an electric field. In addition to the histologic muscle changes seen after EP, several mice were transiently lame in the pelvic limbs the day after EP, but subsequently returned to a normal gait and stance thereafter.

We chose C3H/HeJ mice in this study based on previously documented gross toxicity²¹ and our previous experience suggesting that they were more sensitive to IL-12 liver toxicity than other commonly used strains of inbred mice. Concerns about the well documented (16) defective TLR4 signaling in C3H/HeJ mice were not thought to be an issue because TLR4 signaling in mice appears to serve primarily as a lipopolysaccharide (LPS) response pathway. Thus, C3H/HeJ mice are immunologically normal, except for their inability to respond to LPS and to counter Gram negative infection²². Liver and immune changes were detected in this study, but are not thought to be strain-specific.

Liver changes have been described before with rIL-12 therapy²¹. Similar to our findings, mice in previous rIL-12 studies had foci of hepatocellular necrosis with aggregates of Kupffer cell hyperplasia. In this study we have also noted occasional neutrophil and lymphocytes interspersed within the aggregates of Kupffer cells in the acute treatment groups. Lesions in the mice in this study were mild to minimal and transient. The number of lesions correlated with minimal elevations in ALT, but we found no increase in alkaline phosphatase (ALP) and no decrease in albumin (ALB) as was previously seen in rIL-12 toxicity²¹. We chose not to determine levels of aspartate transaminase (AST) because this enzyme is also elevated in cases of muscle damage and is therefore not liver-specific. If liver toxicity were a concern, our results suggest that monitoring serum levels of ALT during therapy would be indicated.

Immune suppression and suppressed leukocyte counts have also been described with IL-12 therapy²¹. In our study, both total white cell counts and individual absolute leukocyte counts were decreased after treatment with ttIL-12. Mean absolute leukocyte counts for neutrophils, lymphocytes, monocytes, and eosinophils never decreased significantly from control mice. Mean total WBC did decrease significantly ($p < 0.05$) from control levels on days three and seven in mice treated with 5 μg of ttIL-12. Furthermore, in the 5 μg ttIL-12 group there were two mice that developed major infectious diseases; one mouse also had concurrent severe DCC which may have been a significant stressor predisposing the mouse to pyelonephritis (or pyelonephritis may have predisposed to DCC); the other mouse had moderate to severe cholangiohepatitis. Since no other mice in the study developed serious infectious disease, there is a possibility that mega-dose ttIL-12 may cause clinically relevant immune suppression. Conversely, at therapeutically relevant doses (1 μg), ttIL-12 EGT is unlikely to cause serious immunosuppression. Nevertheless, in addition to monitoring ALT, we suggest monitoring WBC during therapy – especially if combined with immunosuppressive chemotherapeutics.

DCC was the most serious problem potentially linked to ttIL-12 EGT. Although both of the females with clinical signs attributed to DCC (death and congestive heart failure) were well within the reported 81–89 day range for development of DCC in female C3H/HeJ mice²³, DCC seen in the 100-day-old male mouse (which did not have signs of CHF) was well before the normal onset of 292–465 days reported previously²³. No other mice in the study developed detectable DCC suggesting that this 16% premature incidence in the mega-dose male mice may not have been significant. Nevertheless, until additional studies are done in

mice that are not predisposed to DCC, mega-doses of ttIL-12 would be contraindicated in subjects with similar genetic predisposition.

DCC is common in many strains of inbred mice²⁴. In C3H mice, DCC is caused by a mutation in the *ABCC6* gene leading to deficiency of its protein product, MRP6²⁵. MRP6 is expressed primarily in the liver and kidney but also exists in many other tissues throughout the body, and is in the family of ABC transporters. It has long been known that DCC can be triggered in susceptible mice by a variety of stimuli including: female sex – particularly in breeders, high fat diets, infectious agents^{26, 27}, hormonal status^{23, 28, 29}, diet²³, and freeze-thaw injury (20). In this study, we found that ttIL-12 EGT also appears to hasten the onset of DCC in C3H/HeJ mice.

In summary, we can conclude that ttIL-12 EGT using low-voltage, long-duration pulses is safe and well-tolerated at therapeutically relevant dosages. Mild muscle changes seen after IM EP are unlikely to be a problem in humans given the small area electroporated. Transient acute decreases in total WBC may suggest possible mild immune suppression, so vigilant patient monitoring for infectious disease and serial CBCs would be prudent. However, no infectious diseases were seen in study mice at the clinically relevant dose of 1 µg ttIL-12. Likewise, DCC was not a problem in the 1 µg therapeutic dosage group. However, several mice (three of twelve, or 25%) were affected in the mega dose (5 µg) group at day 30, one of which presumably died of congestive heart failure secondary to DCC. Thus, until additional information is available, people with *ABCC6* gene defects or patients with Pseudoxanthoma elasticum (a heritable disorder of the connective tissue, caused by defective *ABCC6* gene) should be excluded from treatment with mega-dose ttIL-12 EGT. Finally, no effect of ttIL-12 EGT on wound healing was seen – even at a dosage twenty times greater than those likely to be used clinically. Thus, given the safety of this treatment modality, and superiority to wild-type IL-12 therapy (Cutrera, submitted manuscript) we strongly recommend proceeding to phase I trials.

Acknowledgments

This investigation was partially supported by the National Institutes of Health under Ruth L. Kirschstein T-32 National Research Service Award and R01 grant #R01CA120895. The authors thank Michael Fons of Inovio Biomedical Corp. for supplying the Medpulsar™ electroporator and electrodes used in this study.

REFERENCES

1. Yoshida A, Koide Y, Uchijima M, Yoshida TO. IFN-gamma induces IL-12 mRNA expression by a murine macrophage cell line, J774. *Biochem Biophys Res Commun.* 1994; 198(3):857–861. [PubMed: 7906942]
2. Tannenbaum CS, Tubbs R, Armstrong D, Finke JH, Bukowski RM, Hamilton TA. The CXC chemokines IP-10 and Mig are necessary for IL-12-mediated regression of the mouse RENCA tumor. *J Immunol.* 1998; 161(2):927–932. [PubMed: 9670971]
3. Trinchieri G. Interleukin-12: a cytokine produced by antigen-presenting cells with immunoregulatory functions in the generation of T-helper cells type 1 and cytotoxic lymphocytes. *Blood.* 1994; 84(12):4008–4027. [PubMed: 7994020]
4. Brunda MJ, Luistro L, Warriar RR, Wright RB, Hubbard BR, Murphy M, et al. Antitumor and antimetastatic activity of interleukin 12 against murine tumors. *J Exp Med.* 1993; 178(4):1223–1230. [PubMed: 8104230]
5. Nastala CL, Edington HD, McKinney TG, Tahara H, Nalesnik MA, Brunda MJ, et al. Recombinant IL-12 administration induces tumor regression in association with IFN-gamma production. *J Immunol.* 1994; 153(4):1697–1706. [PubMed: 7913943]
6. Cohen J. IL-12 deaths: explanation and a puzzle. *Science.* 1995; 270(5238):5908.

7. Leonard JP, Sherman ML, Fisher GL, Buchanan LJ, Larsen G, Atkins MB, et al. Effects of single-dose interleukin-12 exposure on interleukin-12-associated toxicity and interferon-gamma production. *Blood*. 1997; 90(7):2541–2548. [PubMed: 9326219]
8. Carson WE, Yu H, Dierksheide J, Pfeffer K, Bouchard P, Clark R, et al. A fatal cytokine-induced systemic inflammatory response reveals a critical role for NK cells. *J Immunol*. 1999; 162(8):4943–4951. [PubMed: 10202041]
9. Li S, Zhang X, Xia X. Regression of tumor growth and induction of long-term antitumor memory by interleukin 12 electro-gene therapy. *J Natl Cancer Inst*. 2002; 94(10):762–768. [PubMed: 12011227]
10. Daud AI, DeConti RC, Andrews S, Urbas P, Riker AI, Sondak VK, et al. Phase I trial of interleukin-12 plasmid electroporation in patients with metastatic melanoma. *J Clin Oncol*. 2008; 26(36):5896–5903. [PubMed: 19029422]
11. Heller L, Merkler K, Westover J, Cruz Y, Coppola D, Benson K, et al. Evaluation of toxicity following electrically mediated interleukin-12 gene delivery in a B16 mouse melanoma model. *Clin Cancer Res*. 2006; 12(10):3177–3183. [PubMed: 16707618]
12. Muramatsu T, Nakamura A, Park HM. In vivo electroporation: a powerful and convenient means of nonviral gene transfer to tissues of living animals (Review). *Int J Mol Med*. 1998; 1(1):55–62. [PubMed: 9852198]
13. Reed SD, Li S. Electroporation Advances in Large Animals. *Curr Gene Ther*. 2009
14. Li S. Delivery of DNA into tumors. *Methods Mol Biol*. 2008; 423:311–318. [PubMed: 18370209]
15. Trollet C, Scherman D, Bigey P. Delivery of DNA into muscle for treating systemic diseases: advantages and challenges. *Methods Mol Biol*. 2008; 423:199–214. [PubMed: 18370200]
16. Trollet C, Bloquel C, Scherman D, Bigey P. Electrotransfer into skeletal muscle for protein expression. *Curr Gene Ther*. 2006; 6(5):561–578. [PubMed: 17073602]
17. Fedorov VV, Nikolski VP, Efimov IR. Effect of electroporation on cardiac electrophysiology. *Methods Mol Biol*. 2008; 423:433–448. [PubMed: 18370220]
18. Serafini P, De Santo C, Marigo I, Cingarlini S, Dolcetti L, Gallina G, et al. Derangement of immune responses by myeloid suppressor cells. *Cancer Immunol Immunother*. 2004; 53(2):64–72. [PubMed: 14593498]
19. Kiessling R, Wasserman K, Horiguchi S, Kono K, Sjoberg J, Pisa P, et al. Tumor-induced immune dysfunction. *Cancer Immunol Immunother*. 1999; 48(7):353–362. [PubMed: 10501847]
20. Carrio R, Lopez DM. Impaired thymopoiesis occurring during the thymic involution of tumor-bearing mice is associated with a down-regulation of the antiapoptotic proteins Bcl-XL and A1. *Int J Mol Med*. 2009; 23(1):89–98. [PubMed: 19082511]
21. Car BD, Eng VM, Lipman JM, Anderson TD. The toxicology of interleukin-12: a review. *Toxicol Pathol*. 1999; 27(1):58–63. [PubMed: 10367675]
22. Poltorak A, He X, Smirnova I, Liu MY, Van Huffel C, Du X, et al. Defective LPS signaling in C3H/HeJ and C57BL/10ScCr mice: mutations in Tlr4 gene. *Science*. 1998; 282(5396):2085–2088. [PubMed: 9851930]
23. Eaton GJ, Custer RP, Johnson FN, Stabenow KT. Dystrophic cardiac calcinosis in mice: genetic, hormonal, and dietary influences. *Am J Pathol*. 1978; 90(1):173–186. [PubMed: 145807]
24. Korff S, Riechert N, Schoensiegel F, Weichenhan D, Autschbach F, Katus HA, et al. Calcification of myocardial necrosis is common in mice. *Virchows Arch*. 2006; 448(5):630–638. [PubMed: 16211391]
25. Aherrahrou Z, Doehring LC, Ehlers EM, Liptau H, Depping R, Linsel-Nitschke P, et al. An alternative splice variant in Abcc6, the gene causing dystrophic calcification, leads to protein deficiency in C3H/He mice. *J Biol Chem*. 2008; 283(12):7608–7615. [PubMed: 18201967]
26. Gang DL, Barrett LV, Wilson EJ, Rubin RH, Medearis DN. Myopericarditis and enhanced dystrophic cardiac calcification in murine cytomegalovirus infection. *Am J Pathol*. 1986; 124(2):207–215. [PubMed: 3017116]
27. Price P, Eddy KS, Papadimitriou JM, Faulkner DL, Shellam GR. Genetic determination of cytomegalovirus-induced and age-related cardiopathy in inbred mice. Characterization of infiltrating cells. *Am J Pathol*. 1991; 138(1):59–67. [PubMed: 1846266]

28. Lostroh A, Li CH. Deposition induced by hydrocortisone of calcium in the heart tissue of female C3H mice. *Nature*. 1955; 176(4480):504. [PubMed: 13253601]
29. Sparks LL, Rosenau W, Macalpin RN, Daane TA, Li CH. Production of dystrophic calcification of cardiac muscle in mice by hydrocortisone. *Nature*. 1955; 176(4480):503–504. [PubMed: 13253600]

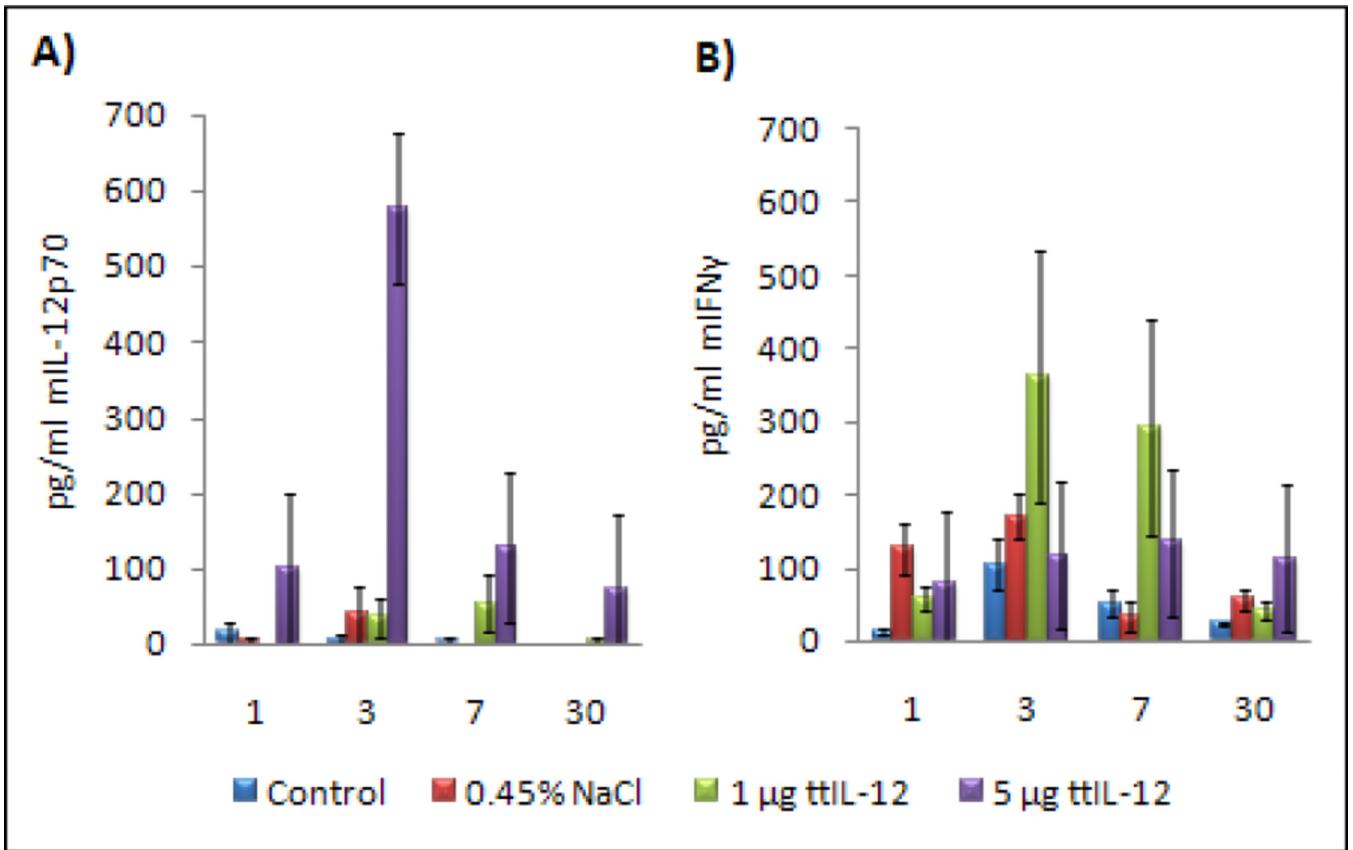


Fig. 1. Optimization of Medpulsor™ electroporation settings and Plasma IL-12 and IFN γ levels after ttIL-12 EGT. A, Comparison of luciferase gene expression after electroporation using different voltage applicators. B, There is no statistical difference ($p > 0.05$) in mean plasma murine IL-12p70 cytokine levels between groups, but trends are illustrated. C, Mean plasma murine IFN γ also were not statistically different between groups ($p > 0.05$), but did trend toward higher levels over time with return to normal. X-axis is the number of days after the IM EGT treatment. Error bars represent standard error of the mean.

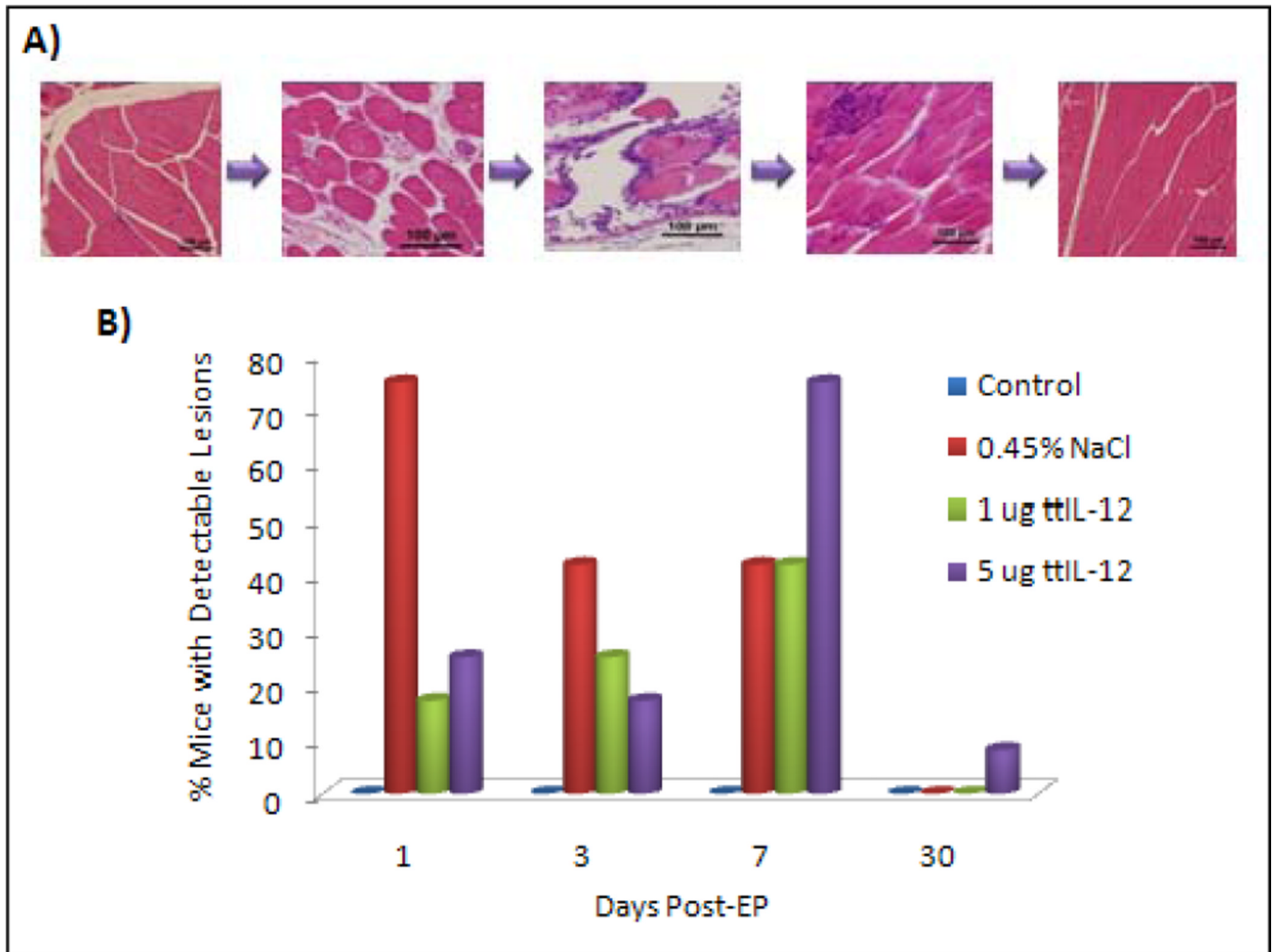
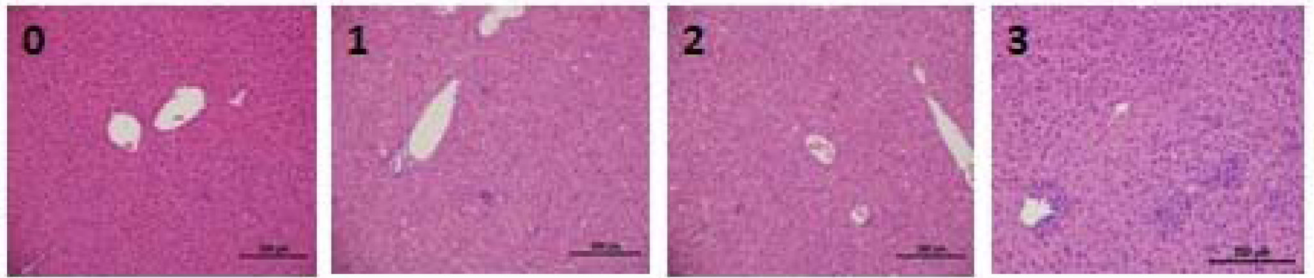
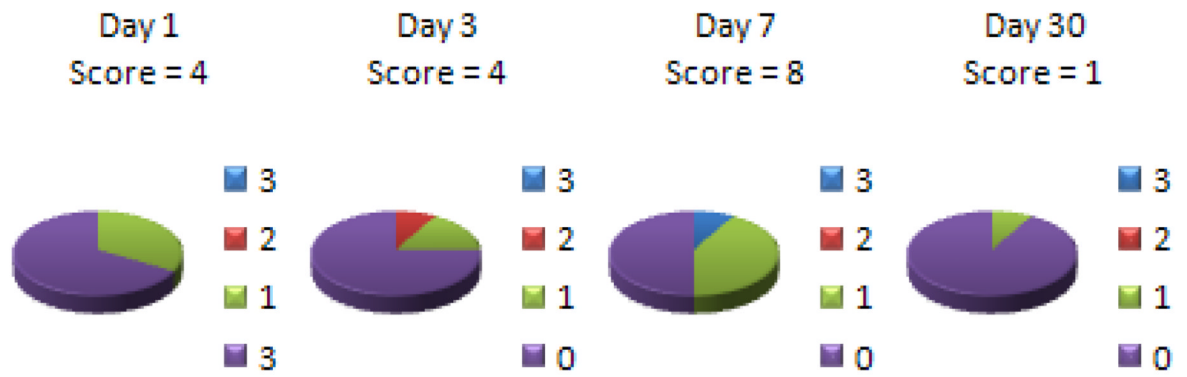


Fig. 2. Muscle damage associated with EP. A, Photomicrographs illustrating the spectrum of muscle damage detected over time. On the left is quadriceps from an untreated mouse illustrating the normal muscle appearance. The next panel is from a mouse sacrificed one day after intramuscular EP demonstrating separation of the endomysium by fibrin and edema. The third panel is from a mouse three days post-EP demonstrating fragmentation, rounding, hyper eosinophilia, and hyalinization of myofibers with a moderate multifocal to coalescing infiltrate of histiocytes and neutrophils. The fourth panel is from a mouse sacrificed seven days post-EP demonstrating resolving muscle damage with early regeneration and multifocal aggregates of histiocytes. The last panel is from a mouse sacrificed on day 30 post-EP illustrating normal musculature. Hematoxylin & eosin staining of paraffin embedded formalin-fixed tissue. 200 \times magnification, bar = 100 μ m. B, Chart illustrating the percentage of mice with detectable quadriceps lesions.

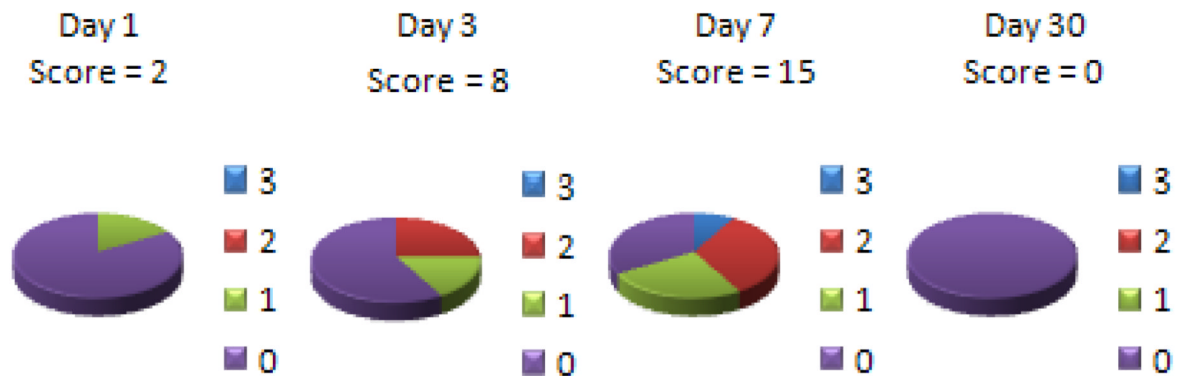
A)



B)



C)



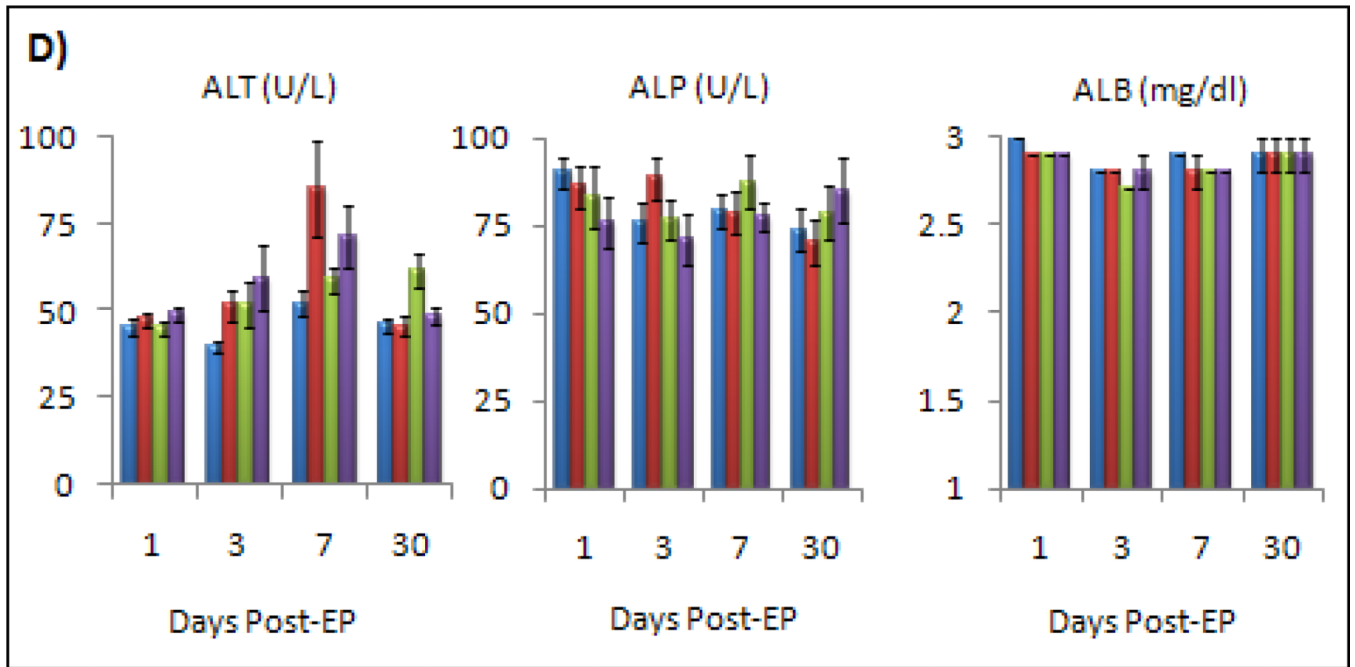
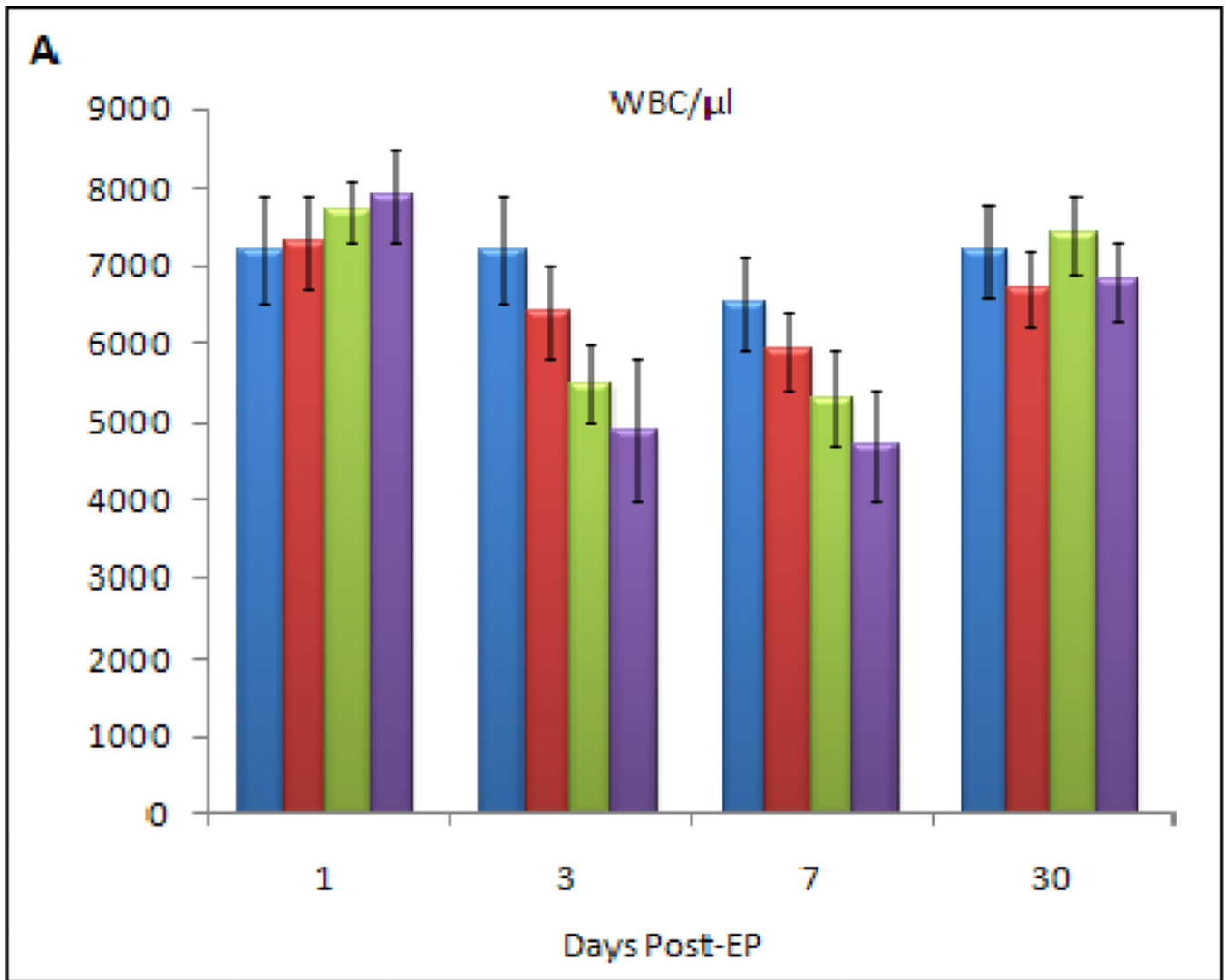
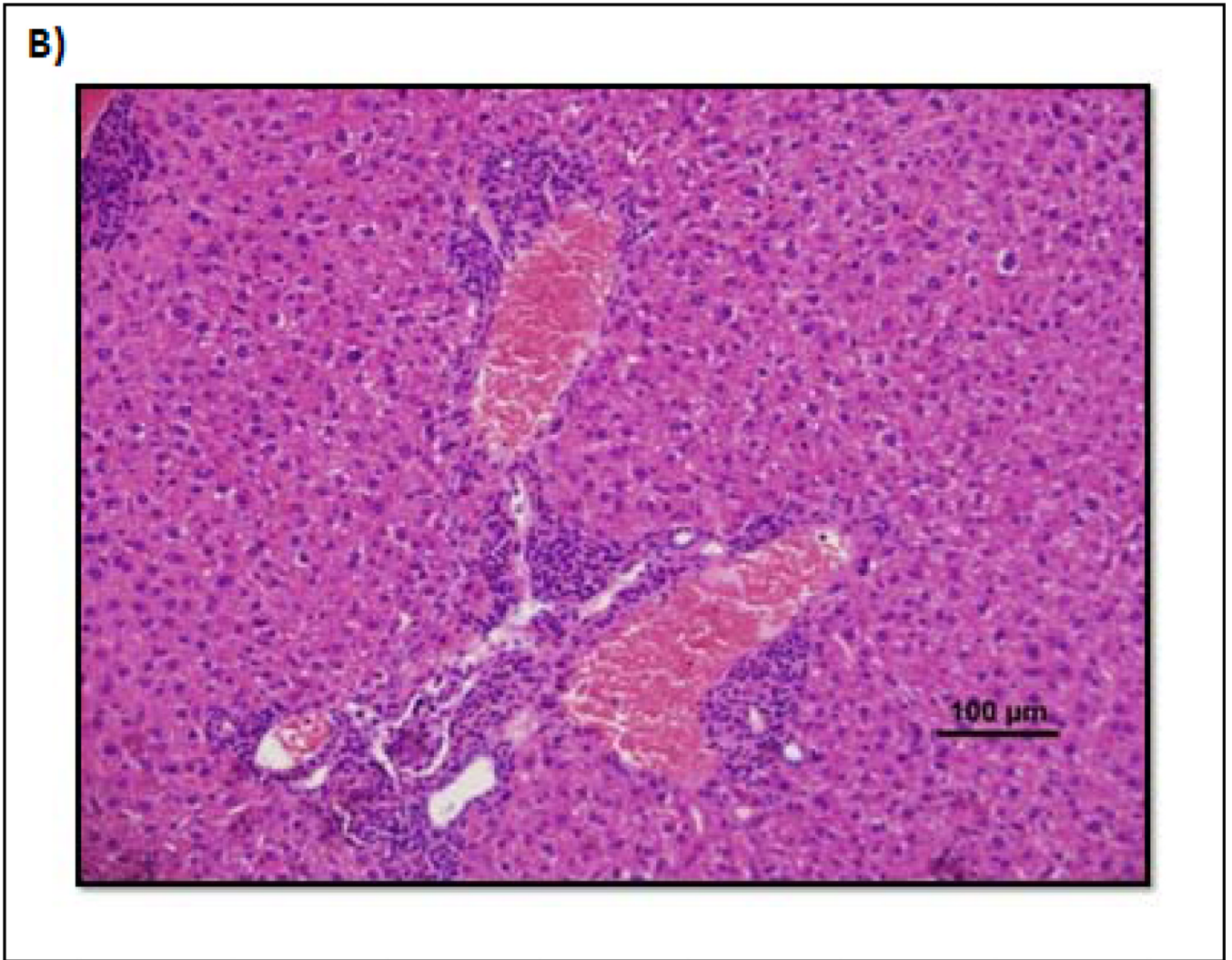


Fig. 3.

Incidence of mild liver toxicity in ttIL-12 treated mice. A, Examples of liver histopathology for the liver toxicity scoring system used indicating that in all cases the toxicity was mild. The panel on the left illustrates non-affected liver. The second panel is consistent with a grade 1 score characterized by 1 lesion per 100 × field. The third panel is a grade 2 liver with 1–3 lesions per 100 × field. The fourth panel is a grade 3 liver with 3–8 lesions per 100 × field. Lesions consisted of small foci of hepatocellular necrosis with Kupffer cell hyperplasia with sporadic neutrophils & lymphocytes. Hematoxylin and eosin staining of paraffin-embedded formalin-fixed tissue. 100 × magnification, bar = 200 μm. B, Incidence of liver lesions by lesion score and total group score (number at the top of the pie chart) for mice treated with 1 μg ttIL-12. C, Incidence of liver lesions by lesion score and total group score (large bold number in the center) for mice treated with 5 μg ttIL-12. D, Plasma levels of liver parameters by group and day. The 0.45% saline treatment group approached statistical significance for ALT on day 7 ($p=0.51$), but all other changes were not statistically significant ($p>0.05$).





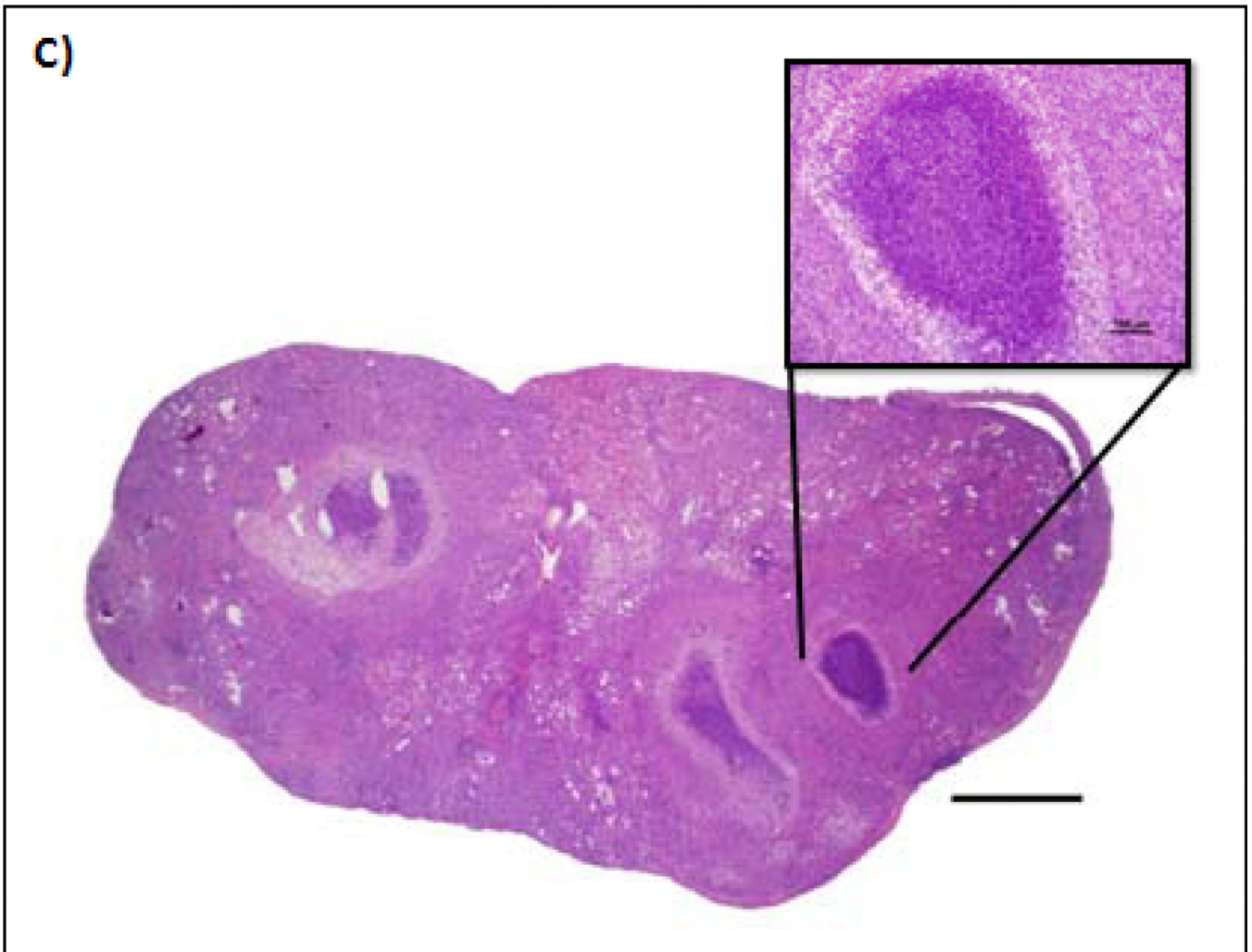


Fig. 4. Changes in total WBC in response to tIL-12 over time. A, Chart depicting the change in total white blood cell count for each group over time. *Indicates significant change in total WBC. B, Photomicrograph from one of the mice in the 30 day 5 μ g treatment group depicting a subacute moderate diffuse pericholangitis or portal hepatitis. C, Kidney photomicrograph from another mouse in the 30 day 5 μ g treatment group depicting a severe, diffuse, subacute to chronic, pyogranulomatous pyelonephritis effacing the entire kidney. Hematoxylin and eosin staining of paraffin-embedded formalin-fixed tissue.

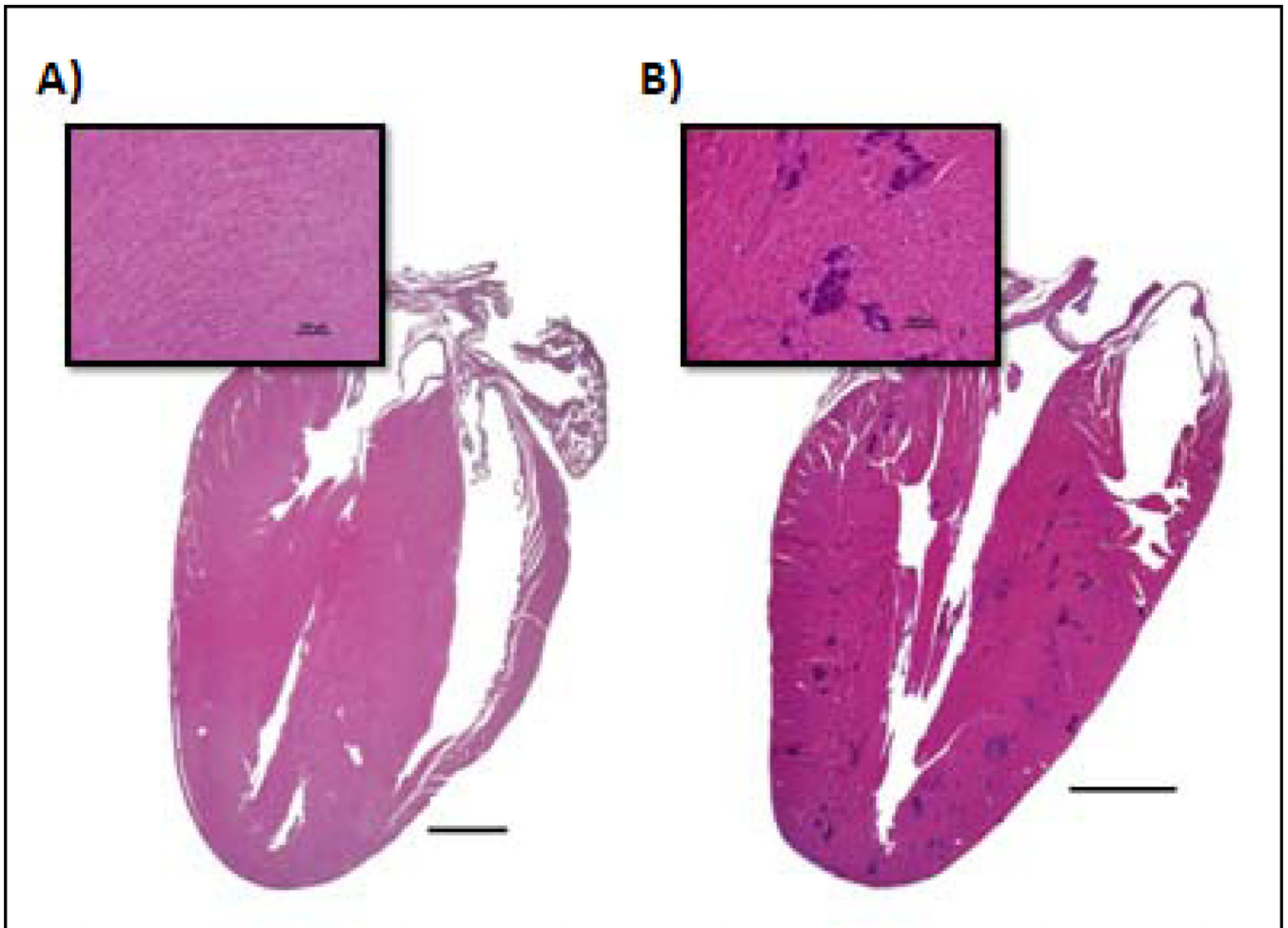


Fig. 5. Photomicrographs comparing an untreated mouse heart to a heart with dystrophic cardiac calcification (DCC). A, Normal heart section with inset of the myocardium demonstrating no evidence of myocardial mineralization. B, Section and inset from a mouse demonstrating moderate, multifocal myocardial mineralization (intensely basophilic foci) throughout the ventricular free wall and interventricular septum characteristic of DCC. Hematoxylin and eosin staining of paraffin-embedded formalin-fixed tissue.

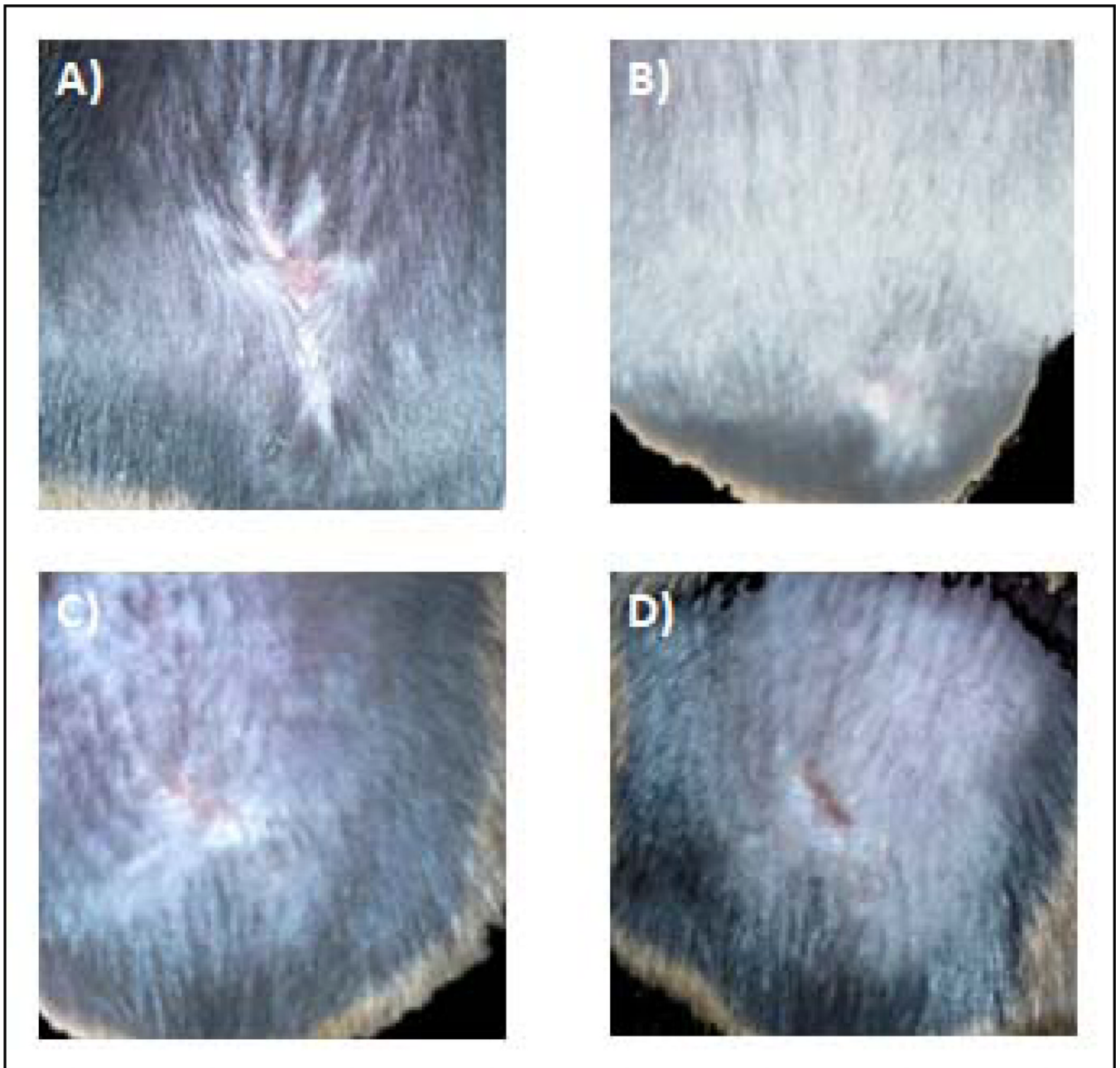


Fig. 6.

Therapy with tumor-targeted interleukin 12 does not delay wound healing. Incision healing seven days after surgery in the untreated control group (A) and the ttIL-12 group (B). There was no significant difference in the time to complete epithelialization between the control and ttIL-12 EGT groups ($p=0.54$)